Journal of Physics: Conference Series

Low-temperature performance of semiconducting asymmetric nanochannel diodes

To cite this article: Y Akbas *et al* 2017 *J. Phys.: Conf. Ser.* **906** 012001

EDISON
IOP Publishing
IOP Conf. Series: Journal of Physics: Conf. Series **906** (2017) 012001 doi:10.1088/1742-6596/906/1/012001

Low-temperature performance of semiconducting asymmetric nanochannel diodes

Y Akbas[1], G R Savich[1], A Jukna,[1,2] T Plecenik[3], P Ďurina[3], A Plecenik[3], G W Wicks[1] and Roman Sobolewski[1]

[1]University of Rochester, Rochester, NY 14627-0231, USA
[2]Vilnius Gediminas Technical University, Vilnius LT-10223, Lithuania
[3]Comenius University, SK-84248 Bratislava, Slovakia

E-mail: roman.sobolewski@rochester.edu

Abstract. We present our studies on fabrication and electrical and optical characterization of semiconducting asymmetric nanochannel diodes (ANCDs), focusing mainly on the temperature dependence of their current–voltage (*I–V*) characteristics in the range from room temperature to 77 K. These measurements enable us to elucidate the electron transport mechanism in a nanochannel. Our test devices were fabricated in a GaAs/AlGaAs heterostructure with a two-dimensional electron gas layer and were patterned using electron-beam lithography. The 250-nm-wide, 70-nm-deep trenches that define the nanochannel were ion-beam etched using the photoresist as a mask, so the resulting nanostructure consisted of approximately ten ANCDs connected in parallel with 2-µm-long, 230-nm-wide nanochannels. The ANCD *I–V* curves collected in the dark exhibited nonlinear, diode-type behavior at all tested temperatures. Their forward-biased regions were fitted to the classical diode equation with a thermionic barrier, with the ideality factor *n* and the saturation current as fitting parameters. We have obtained very good fits, but with *n* as large as ~50, suggesting that there must be a substantial voltage drop likely at the contact pads. The thermionic energy barrier was determined to be 56 meV at high temperatures. We have also observed that under optical illumination our ANCDs at low temperatures exhibited, at low illumination powers, a very strong photoresponse enhancement that exceeded that at room temperature. At 78 K, the responsivity was of the order of 10^4 A/W at the nW-level light excitation.

1. Introduction

Intrinsic nanostructures exhibit unique physical properties that are a direct consequence of their nanoscale parameters and the quantum mode of operation, in contrast to scaled-down versions of well-known conventional devices. One of the best-known examples is a nonlinear, asymmetric nanochannel diode (ANCD), also called a self-switching diode (SSD), invented in 2004 by Song *et al.* [1]. Unlike conventional (e.g., *p-n*) diodes, the ANCD performance is not based on the junction barrier; instead, it produces diode-like characteristics through nonlinear carrier transport in a depletion-controlled nanochannel. Since depletion control is purely geometrical and the device itself has a planar geometry, there is room for flexibility in terms of material selection and device design. In terms of the applications, when combined with coupling antennas, ANCDs act as reliable and sensitive THz detectors [2], as well as (based on Monte Carlo simulations) THz generators [3]. They have also been proposed as ultrafast logic gate operators [4] and most recently have been demonstrated as ultrasensitive optical detectors [5].

To maximize carrier transport, most ANCDs are fabricated on wafers with a two-dimensional electron gas (2DEG) layer. Therefore, the ballistic transport enables their ultrafast operation or, equivalently, THz-frequency bandwidth. Our research presented here focuses on exploiting low-temperature performance ANCDs with strongly nonlinear current–voltage (*I–V*) characteristics and demonstrates that they exhibit a very large gain at ultralow optical excitations [5]. The latter makes them promising for single-photon detection applications.

2. Fabrication and Experimental Setup

A schematic cross section of an actual wafer used to fabricate our devices is shown in Figure 1a. It is a GaAs/AlGaAs quantum-well heterostructure grown in-house by molecular-beam epitaxy on a semi-insulating GaAs substrate that exhibits a 2DEG layer at the GaAs/AlGaAs interface, ~50 nm below the surface. The heterostructure cross section in Figure 1a is overlaid with an atomic force microscopy (AFM) profile from an actual fabricated device, showing that the ~65-nm trench etching is deep enough to isolate the 2DEG layer. A sketch of a fabricated device chip is shown in Figure 1b. The entire structure consists of contact pads (blue areas) with 20-nm-thick Pt metallization and a mesa structure (gray region) etched out to isolate the ANCDs from their surroundings. Finally, the actual nanostructures (black U shapes) are fabricated at the mesa center. Using electron-beam lithography patterning and the resist as a mask, nanometer-width trenches are etched down below the 2DEG level (see Figure 1a) via ion-beam etching. Figure 1c presents an AFM top view image of completed ANCDs. For practical purposes, the ends of trenches bend away from each other. Typically, about ten devices connected in parallel were fabricated, each having a <2-µm-long, ~230-nm-wide nanochannel. The trenches were ~65 nm deep (see Figure 1a).

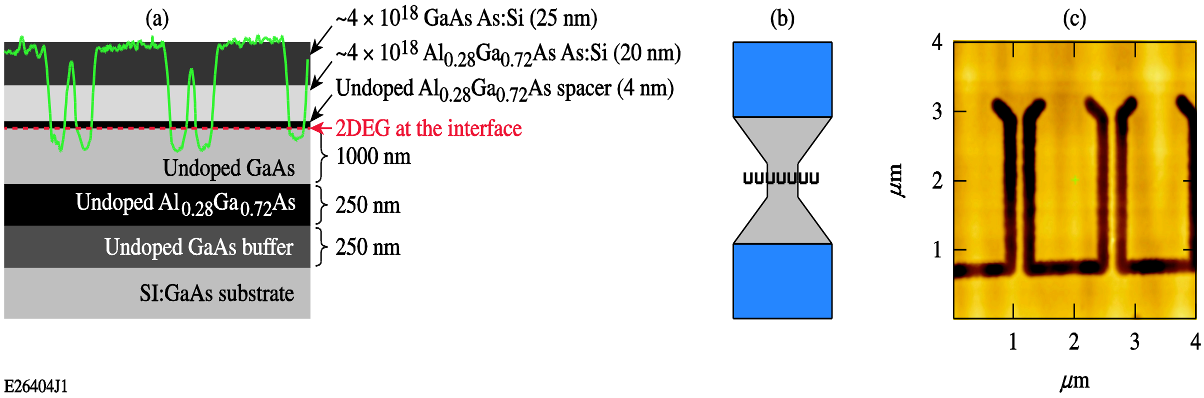

Figure 1. (a) Schematics of a GaAs-based heterostructure with a 2DEG layer ~50 nm below the surface. The heterostructure cross section has been overlaid with an AFM profile of the actual etched ANCD nanostructure. (b) Sketch of a test structure with ANCDs in parallel at the centre of the mesa (black U-shaped structures). (c) An AFM image of a section of the completed ANCDs.

The ANCD *I–V* characteristics have been collected by biasing the device with a constant-voltage source and measuring the transport current under both the dark and light illumination conditions. The device under test was placed inside a liquid nitrogen cryostat with glass windows for optical access, enabling us to perform measurements in the temperature range between 78 K and 300 K. The cryostat also acted as a shield to block stray light. For optical excitation experiments, we used a train of 800-nm-wavelength, 100-fs-wide pulses of light generated by a commercial Ti:sapphire laser with a 76-MHz repetition rate. Using a bank of neutral-density attenuators, different excitation levels from 1 mW to 1 nW could be achieved. A spot size of optical excitation was selected to be 20 µm to ensure uniform optical power delivery to our ANCDs connected in parallel.

3. Results and Discussion

The smaller of the two insets in Figure 2 presents a set of the ANCD *I–V* curves collected at different temperatures *T* between room and liquid nitrogen temperatures. We note that our device exhibits highly nonlinear characteristics and the nonlinearity, as well as the asymmetry of the *I–V* curve, increases with a decrease in temperature. In addition, above ~2.5 V of bias, the traces level off as electrons in the nanochannel reach saturation with a velocity of the order of 10^7 cm/s, corresponding to the ballistic transport. Interestingly, the saturation current level does not simply scale with temperature, which will require further research. At the negative bias, below ~ –2.5 V, the leakage current starts to increase, likely because of the ballistic transport along, this time, a depleted nanochannel.

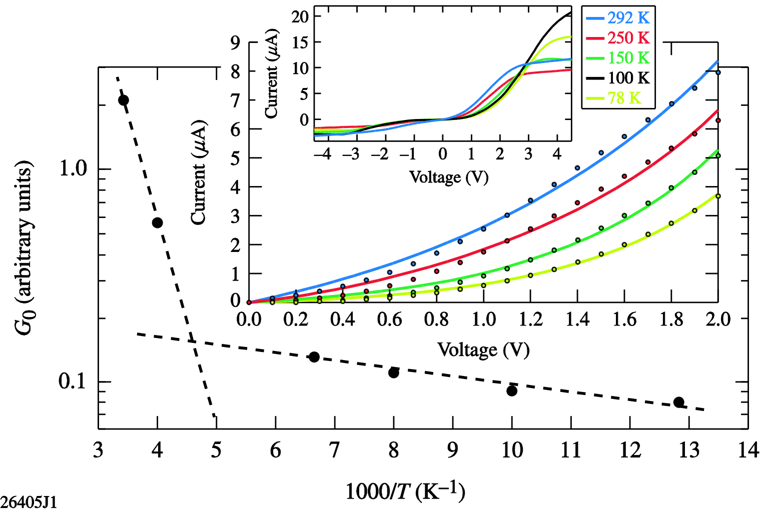

E26405J1

Figure 2. Differential conductivity G_0 plotted versus reciprocal temperature (large black dots) with dashed black lines indicating two regimes of the thermionic electron transport. The smaller inset presents *I–V* characteristics of our ANCD measured at different temperatures (see legend). The larger inset shows forward-biased parts of the same characteristics as the ones in the smaller inset (dots) overlaid with numerical fits (solid lines) based on Eq. (1).

The larger inset in Figure 2 presents forward-biased parts (0- to 2-V regions; dots) of the same *I–V* characteristics as shown in the smaller inset, but now overlaid with fits (solid lines) based on the diode equation analog to the Schottky junction equation, i.e., the one that includes a thermionic barrier:

$$I = I_0 e^{-\phi_{\text{barrier}}/kT}\left(e^{qV/nkT} - 1\right), \qquad (1)$$

where I_0 is a constant corresponding to the saturation current, ϕ_{barrier} is the thermionic barrier energy, and *n* is the ideality factor. Clearly, the fits are very good at all tested temperatures ($R^2 > 0.99$); however, we had to use *n* as large as ~50. The latter is physically unrealistic and must indicate that there is a very large voltage drop at the contact pads, or, possibly, it might be related to an extra voltage drop across the trenches.

Finally the zero-bias differential conductance $G_0 = \mathrm{d}I/\mathrm{d}V$ at $V = 0$ (main panel in Figure 2) is extracted from each *I–V* curve and plotted as a function of reciprocal temperature in a semi-logarithmic scale. The observed behavior indicates the existence of a thermionic energy barrier with $\phi_{\text{barrier}} = 56$ meV at high temperatures that becomes strongly suppressed ($\phi_{\text{barrier}} = 10$ meV) below ~200 K. Therefore, we believe that at temperatures close to room temperature and near-zero bias, our depleted nanochannel represents a thermionic barrier that can be spontaneously/thermally negotiated by carriers as the bias voltage increases, in a way similar to the case of Schottky junctions. At low temperatures, the barrier is much lower and transport becomes ballistic.

Following our earlier research [5], we also performed optical characterization of our ANCDs. We measured the photocurrent's dependence on the incident optical power and then calculated the responsivity. Analogous to our earlier observations, the devices presented here also exhibit a dramatic increase in responsivity as the incident optical power is decreased. The same trend is observed at both room and low temperatures; however, at low temperatures the responsivity increase becomes a steeper function of the optical power, as is shown in Figure 3. We expect that at the single-photon power level (SP point in Figure 3), the responsivity should reach 25000 A/W at 78 K, which should be well within the reach of our next-generation ANCDs. The single-photon level has been calculated to be ~19 pW, corresponding to an average of one photon per 100-fs pulse with an 800-nm wavelength and a 76-MHz repetition rate generated by our laser. Equivalent detection efficiency indicates that for a single absorbed photon, ~1500 electrons should pass through the nanochannel.

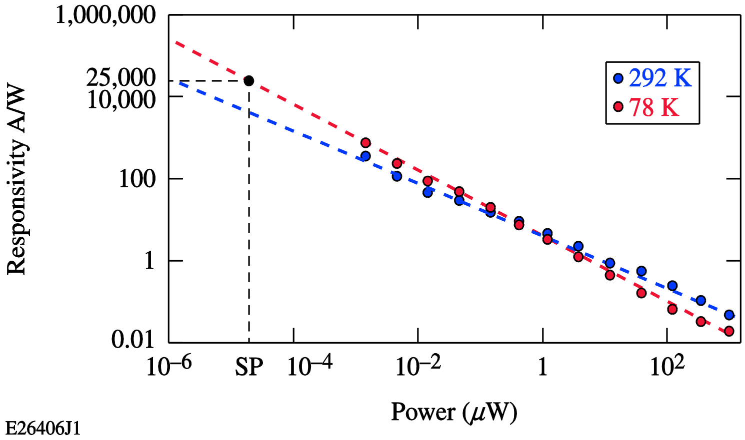

Figure 3. Responsivity versus incident optical power for an ANCD tested at room and liquid nitrogen temperatures (dots). The dashed lines are the linear fits to experimental values. The black dot represents the calculated single-photon (SP) illumination level.

4. Conclusions

We have performed systematic studies of the low-temperature performance of ANCDs fabricated in the GaAs/AlGaAs heterostructure with a 2DEG layer. Our ANCDs were characterized by nonlinear *I–V* characteristics that could be very well fitted using the standard diode equation with a thermionic barrier term. The zero-voltage differential conductivity extracted from the *I–V* curves demonstrated that at high temperatures ϕ_{barrier} = 56 meV and decreased substantially (to the 10-meV value) at temperatures below ~200 K. Our optical excitation experiments confirmed the earlier-observed existence of dramatic responsivity enhancement at very low optical powers incident upon the device; this effect was somewhat enhanced at low temperatures. The measured responsivity reached ~10^4 A/W at nW-level optical excitation at 78 K. With strongly suppressed dark currents at low temperatures, cryogenic ANCDs look to be promising candidates for single-photon–level detectors.

Acknowledgements

The authors thank M. Mosko for valuable discussions. This work was supported in part by the PumpPrimerII Program at the University of Rochester. AJ thanks the Baltic-American Freedom Foundation for their financial support.

References

[1] Song A M, Maximov I, Missous M and Seifert W 2004 *Physica E* **21** 1116
[2] Balocco C, Kasjoo S R, Lu X F, Zhang L Q, Alimi Y, Winnerl S and Song A M 2011 *Appl. Phys. Lett.* **98** 223501
[3] Mateos J, Vasallo B G, Pardo D and González T 2005 *Appl. Phys. Lett.* **86** 212103.
[4] Song A M, Missous M, Omling P, Maximov I, Seifert W and Samuelson L 2005 *Appl. Phys. Lett.* **86** 042106
[5] Akbas Y, Stern A, Zhang L Q, Alimi Y, Song A M, Iñiguez-de-la-Torre I, Mateos J, González T, Wicks G W and Sobolewski R 2015 *J. Phys.: Conf. Ser.* **647** 012013